Acta Crystallographica Section A
Foundations of Crystallography
ISSN 0108-7673

Received 27 October 2004
Accepted 1 February 2005

Intensity of *N*-beam X-ray diffraction: kinematical theory for a small crystal

Shijo Nagao‡

Department of Physics, Kyushu University, Fukuoka 812-8581, Japan. Correspondence e-mail: shijo.nagao@hut.fi

For a small and ideally imperfect crystal, a method for calculating *n*-beam X-ray diffraction intensities has been developed on the basis of macroscopic intensity exchanges among the beams. This kinematical formulation results in a set of simultaneous equations that can be solved by numerical calculation. To validate the macroscopic formulae, the Darwin intensity transfer equations, which describe microscopic interactions by both diffraction and absorption, are integrated on a spherical crystal. With the hypotheses that one beam contributes to other beams as proportional to its observed intensity, the macroscopic and microscopic formulations are proved to be equivalent; quantitative evaluation of the *n*-beam effect thereby becomes available for practical experiments using a specimen with finite cross section of X-ray absorption. Examples of the ψ-scan simulation on Si 111 and 222 are presented to characterize the present method, demonstrating the reasonable behaviour of the observed diffraction intensity while the linear absorption coefficient and the specimen size are varied.

1. Introduction

Multiple X-ray diffraction by *n*-beam interaction arises when more than one reciprocal-lattice point rests on the Ewald sphere simultaneously. The observed diffraction intensity is modified by the *n*-beam interaction, and the magnitude of the modification is comparable with that caused by absorption and extinction. Moreover, controlling the geometrical arrangement may fail to avoid multiple diffractions, since the probability of encountering the phenomenon is higher for X-rays with shorter wavelength, which is generally recommended to reduce absorption. Therefore, some numerical methods for quantitative evaluation of the effect are required for accurate data collection.

The knowledge of this phenomenon in terms of either the kinematical or the dynamical theory of X-ray diffraction has been reviewed by Chang (1984), and recently revived by Authier (2003). Although much progress has been achieved in dynamical theory (Thorkildsen & Larsen, 2002; Okitsu, 2003), the kinematical theory still has an advantage in its simplicity for experimental studies that treat large numbers of beams (Tanaka & Saito, 1975; Hauback *et al.*, 1990; Tanaka *et al.*, 1994). In this article, we revive this kinematical theory to treat the phase-independent part of the phenomena, so-called *Umweganregung* and *Aufhellung*.

For planar shaped crystals with larger size than the cross section of the incident beam, Moon & Shull (1964) utilized the Darwin intensity transfer equations. The beam intensities inside the crystal are described as a function of the length of the path on which the beam has travelled. As shown in Fig. 1(*a*), the path lengths at a point depend on only the penetration depth x from the surface. This reduces the intensity transfer equations to normal differential equations of first order with simple boundary conditions, and thereby the intensities can be approximated by the Taylor-series expansion. The approximation up to the second order has commonly been accepted to interpret the experimental results, *e.g.* Coppens (1968). After the strict solutions had been given for a few special cases at n = 2, 3, 4, 6 (Zachariasen, 1965), the formal solution of the equations for unlimited n was derived by Parente & Caticha-Ellis (1974) in the infinite order of the series expansion, and then applied in practice (Parente *et al.*, 1994; Mazzocchi & Parente, 1994).

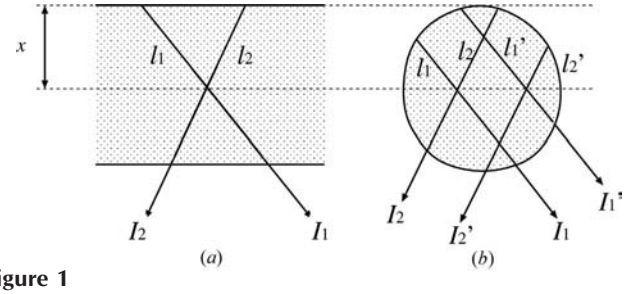

Figure 1
X-ray beam paths through a specimen crystal. The intensities of the diffracted beams are written as I_1 and I_2. (*a*) For a planar crystal, the path length l_i is a function of the penetration depth x: $l_i = x/\gamma_i$, where γ_i denotes the direction cosine to the normal to the crystal surface. (*b*) For a spherical crystal, there is no explicit relation among the path lengths. Belonging to the same beam, two beam paths, l_i and l_i' differ even at the same depth x; therefore, $I_i \neq I_i'$.

‡ Present address: Department of Materials Science and Engineering, Helsinki University of Technology, Espoo 6200, Finland.

In contrast, the application of the equations to a small crystal bathed in incident X-rays has not been established. The path lengths in a small spherical crystal have no clear relation among them (see Fig. 1*b*). The expression remains in partial differential equations on the three-dimensional volume, and the boundary conditions cannot be simplified. No solution of these equations is known, though selecting a small and spherical crystal for a diffraction experiment suppresses the absorption effect and improves the angular resolution.

On the other hand, Soejima *et al.* (1985) have presented an expression of *n*-beam diffraction intensity for a small spherical crystal without solving the intensity transfer equations. Instead, they have adopted simple simultaneous equations also based on the kinematical theory. The final expression is nearly equal to the second-order Taylor-series approximation of the intensity transfer equations, especially for the *Umweganregung* case (Renninger, 1937). The validity of the method has experimentally been proved in the application to small crystals bathed in incident X-rays, for both *Umweganregung* and *Aufhellung* cases (Okazaki, Ohe & Soejima, 1988; Okazaki, Soejima *et al.*, 1988). But the derivation process and the assumptions on which the calculation is based are not clear so that it is difficult to discuss the approximation level. Moreover, the fundamental simultaneous equations are not symmetrical for the intensities of each beams. The method thus contains some ambiguity in its foundation in spite of its effectiveness.

In the next section, we firstly revise the theory given by Soejima *et al.* (1985) from the viewpoint of symmetry. The resulting formulae are given in matrix form, as a macroscopic intensity equation. Then, to examine the microscopic foundation of the formulae, we attempt to integrate the intensity transfer equations for small spherical crystals. With a simple hypothesis, it is confirmed that the integrated equations are equivalent to the macroscopic equations mentioned above. Some example calculations of the ψ-scan profile on Si 111 and 222 are presented to characterize the present theory on the effect of the hypotheses and the absorption coefficient.

2. Kinematical theory of *n*-beam interaction

2.1. Macroscopic formulation

The formulation of the three-beam case in Soejima *et al.* (1985) starts with the equation

$$I_{\mathbf{h}} = (I_0 - I_{\rm op}) r_{\mathbf{h}} N_{\mathbf{h}}, \tag{1}$$

where I_0, $I_{\mathbf{h}}$ and $I_{\rm op}$ are the intensities of the incident beam, and primary and secondary diffracted beam, respectively. Kinematical reflectivity including the Lorentz–polarization factor is denoted by $N_{\mathbf{h}}$ and the transmission factor of the crystal by $r_{\mathbf{h}}$.

This expression implies that the intensity of the incident beam is modified by the secondary diffraction, and the primary diffraction intensity is proportional to the modified intensity. Although the idea is effective, (1) is difficult to interpret; the direct subtraction of the two intensities is unreasonable since the secondary diffraction $I_{\rm op}$ has no relation to $N_{\mathbf{h}}$, the reflectivity of the primary diffraction. Furthermore, the primary diffraction should also affect the incident beam through the second-order extinction effect. These problems are caused by mixing the observed intensities with the interactions among the beams indistinctly. To construct symmetrical formulae on the intensities in the *n*-beam case, we thus need to figure out such primitive interactions.

The kinematical reflectivity of the diffraction from the *j*th beam to the *i*th beam can be written as

$$N_{ij} \propto |F(\mathbf{h}_{ij})|^2 {\rm Lp}, \tag{2}$$

where F is the crystal structure factor specified by the reciprocal vector $\mathbf{h}_{ij} \equiv \mathbf{h}_i - \mathbf{h}_j$ and Lp is the Lorentz–polarization factor. Fig. 2 shows the relation between the reciprocal vectors and the wavevectors. According to the idea implied in (1), the contribution to the *i*th beam through the diffraction $\mathbf{h}_{ij}$ can be written as

$$\Delta I_{ij} = N_{ij} I_j, \tag{3}$$

where I_j is the *observed* intensity of the *j*th beam. ΔI_{ij} represents the amount of modification in the *i*th beam intensity, and hence we can add it to I_i without any problem. If we count only elastic coherent scattering, I_j decreases by the contribution ΔI_{ij}. Therefore, total modification of I_i by the *j*th beam is

$$\Delta I_{ij} - I_{ji} = N_{ij} I_j - N_{ji} I_i. \tag{4}$$

The contributions of absorption including inelastic or incoherent scattering will be considered in the next subsection. While I_0 should be regarded not as the incident but as the transmitted intensity, expression (4) is valid for all the beams ($0 \le i, j < n$).

Now we can reckon up all the interactions among the beams. First, we consider the three-beam case as the simplest one, which has six interactions as schematically shown in Fig. 3. Summing up the contributions (4) for each beam, we obtain a set of simultaneous equations:

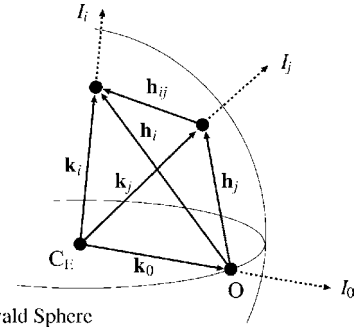

Figure 2
The relation between the reciprocal vectors. The wavevectors denoted by $\mathbf{k}_0$, $\mathbf{k}_i$ and $\mathbf{k}_j$ correspond to the incident, the *i*th and the *j*th beam, respectively. The interaction between the *i*th and the *j*th beams can be represented by the reciprocal vectors of the bidirectional diffraction: $\mathbf{h}_{ij} = -\mathbf{h}_{ji} = \mathbf{h}_i - \mathbf{h}_j$.

$$\begin{cases} I_0 = I^{\rm in} + N_{01}I_1 + N_{02}I_2 - N_{10}I_0 - N_{20}I_0 \\ I_1 = \quad N_{10}I_0 + N_{12}I_2 - N_{01}I_1 - N_{21}I_1 \\ I_2 = \quad N_{20}I_0 + N_{21}I_1 - N_{02}I_2 - N_{12}I_2, \end{cases} \tag{5}$$

where $I^{\rm in}$ is the intensity of the incident X-rays. These simultaneous equations can be transformed to a matrix equation,

$$\mathbf{I}^{\rm out} = \mathbf{I}^{\rm in} + \mathbf{T}\mathbf{I}^{\rm out}, \tag{6}$$

by constructing the matrix $\mathbf{T}$ of the three-beam case as

$$\mathbf{T} = \begin{pmatrix} -(N_{10}+N_{20}) & N_{01} & N_{02} \\ N_{10} & -(N_{01}+N_{21}) & N_{12} \\ N_{20} & N_{21} & -(N_{02}+N_{12}) \end{pmatrix}. \tag{7}$$

The intensities of the incident and diffracted beams are respectively packed into the three-dimensional vectors

$$\mathbf{I}^{\rm in} = \begin{pmatrix} I^{\rm in} \\ 0 \\ 0 \end{pmatrix} \quad \text{and} \quad \mathbf{I}^{\rm out} = \begin{pmatrix} I_0 \\ I_1 \\ I_2 \end{pmatrix}. \tag{8}$$

To get a formal solution of (6), we define a matrix $\mathbf{D}$ as

$$\mathbf{D} = \mathbf{E} - \mathbf{T} = \begin{pmatrix} 1+N_{10}+N_{20} & -N_{01} & -N_{02} \\ -N_{10} & 1+N_{01}+N_{21} & -N_{12} \\ -N_{20} & -N_{21} & 1+N_{02}+N_{12} \end{pmatrix}, \tag{9}$$

where $\mathbf{E}$ is the 3×3 identity matrix. The observed intensities of the diffracted beams can thereby be calculated as

$$\mathbf{I}^{\rm out} = \mathbf{D}^{-1}\mathbf{I}^{\rm in} \tag{10}$$

if $\mathbf{D}$ is a regular matrix. Even in the three-beam case, the actual solution of a diffracted beam is too complicated to be written down explicitly, although it is possible.

To apply these formulae for a general n-beam case, we just redefine $\mathbf{T}$ as an $n \times n$ matrix:

$$T_{ij} \equiv N_{ij} - \delta_{ij}\sum_{k=0}^{n-1} N_{kj}, \tag{11}$$

where δ_{ij} is the Kronecker delta. Cancelled by the subtraction on the diagonal elements, N_{ii}, which is undefined, does not appear in the matrix. Both the intensity vectors should also be extended to n-dimensional ones as

$$\mathbf{I}^{\rm in} = \begin{pmatrix} I^{\rm in} \\ 0 \\ \vdots \\ 0 \end{pmatrix} \quad \text{and} \quad \mathbf{I}^{\rm out} = \begin{pmatrix} I_0 \\ I_1 \\ \vdots \\ I_{n-1} \end{pmatrix}. \tag{12}$$

Equation (6) is still valid for these variables; therefore, the diffraction intensities of a general n-beam case can be obtained by (10), under the condition that the matrix $\mathbf{D}$, which is now written as

$$D_{ij} = \delta_{ij}\left(1 + \sum_{k=0}^{n-1} N_{kj}\right) - N_{ij}, \tag{13}$$

is regular.

The properties of $\mathbf{D}$ determine whether (6) can be solved or not. If we assume $N_{ij} = N_{ji}$ by Friedel's law for the reflectivities of the Bijvoet pair h_{ij} and h_{ji}, $\mathbf{D}$ becomes a symmetric matrix, *i.e.* regular. For X-ray diffraction, it is not practical to neglect the effects of the Lp factor and anomalous dispersion that break the assumption. However, $\mathbf{D}$ is diagonal dominant because we expect $0 \leq N_{ij} \ll 1$. This means that (6) can easily be solved by a proper numerical method, which is still available for large n. Thus, $\mathbf{I}^{\rm out}$ can be calculated by (10), although is not proved to exist in general.

As we see above, a set of diffracted intensities can be calculated in general n-beam cases. It should be noted that the solvable simultaneous equations arise from the macroscopic idea that one beam contributes to other beams as proportional to its observed intensity. The resulting formulae are also macroscopic, and not sufficient for real calculations including the absorption effect. To study the detailed foundations of this method, we will discuss integration of differential equations that describe microscopic interactions.

2.2. Integration of the intensity transfer equations

The intensity transfer equations in the n-beam case (Moon & Shull, 1964) can be summarized as follows with slight changes in notation:

$$\begin{aligned} \frac{{\rm d}I_0}{{\rm d}x} &= -\left(\mu + \sum_{j\neq 0} r_{j0}\right)\frac{I_0}{\gamma_0} + \sum_{j\neq 0} r_{ij}\frac{I_j}{\gamma_j}, \\ \pm\frac{{\rm d}I_i}{{\rm d}x} &= -\left(\mu + \sum_{j\neq i} r_{ji}\right)\frac{I_i}{\gamma_i} + \sum_{j\neq i} r_{ij}\frac{I_j}{\gamma_j}. \end{aligned} \tag{14}$$

Here γ_i denotes the direction cosine of the ith beam. In contrast with the macroscopic formulae described in the previous section, the intensity I_i of the ith beam is not the observed one but a function of the penetration length x from the surface of the specimen crystal (see Fig. 1*a*). The sign on the left-hand side is determined by the orientation of the beam, the plus being for transmission and the minus for reflection. The reflectivity r_{ij} from the jth beam to the ith beam is defined as

$$r_{ij} \equiv Q_{ij}W(\delta\theta), \tag{15}$$

where Q_{ij} is the integrated reflectivity per unit volume and $W(\delta\theta)$ is the mosaic spread function of the specimen.

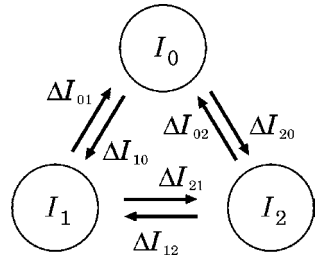

Figure 3
In the three-beam case, there are six interactions between each two of the beams. The difference $\Delta I_{ij} - \Delta I_{ji}$ causes a multiple diffraction effect, even if $N_{ij} = N_{ji}$, which is usually fulfilled for neutron diffraction.

Equations (14) can be regarded as an n-beam extension of Hamilton–Zachariasen's equations that describe the second-order extinction effect on X-ray or neutron diffraction. For a small crystal, Becker & Coppens (1974) wrote the equations as

$$\begin{aligned}\frac{\partial I_0}{\partial x_0} &= -(\mu+\sigma)I_0 + \sigma I_1,\\ \frac{\partial I_1}{\partial x_1} &= -(\mu+\sigma)I_1 + \sigma I_0,\end{aligned} \tag{16}$$

where μ denotes the linear absorption coefficient and the interaction σ has a value proportional to the integrated reflectivity per unit length. The coordinates x_0 and x_1 are along the directions of the incident and diffracted beams, respectively.

We rewrite (14) in the style of (16) because the signs on the left-hand side and the direction cosines are introduced only for planar crystals to reduce the dimension to unity. As we need not distinguish the incident beam from the diffracted one, (14) can be expressed in a unified form:

$$\frac{\partial}{\partial x_i} I_i = -\left(\mu + \sum_{j\neq i} r_{ji}\right) I_i + \sum_{j\neq i} r_{ij} I_j, \tag{17}$$

where $\partial/\partial x_i$ denotes partial differentiation along the direction of the ith beam (Hauback *et al.*, 1990).

To integrate (17), we assume a situation in which a small nearly spherical crystal is fully bathed in the incident X-ray beam. As illustrated in Fig. 4, we consider beam paths in the crystal along the direction of the ith beam, then identify one of the paths by specifying a point $\mathbf{s}$ on the cross section S. The intensity field $I_i(\mathbf{r})$ defined over the crystal can be written as $I_i(\mathbf{s}, x_\mathbf{s})$ on the path $\mathbf{s}$, where $x_\mathbf{s}$ is the penetration length along the path. The intensities at the two ends of the path $\mathbf{s}$ are $I_i(\mathbf{s}, 0)$ and $I_i(\mathbf{s}, l_\mathbf{s})$, respectively, where $l_\mathbf{s}$ is the length of the path. Since the whole surface of the crystal is in the incident beam, the boundary conditions can be written as

$$I_i^{\rm in} = \int_S I_i(\mathbf{s}, 0)\,{\rm d}\mathbf{s} \quad \text{and} \quad I_i^{\rm out} = \int_S I_i(\mathbf{s}, l_\mathbf{s})\,{\rm d}\mathbf{s}, \tag{18}$$

where $I_i^{\rm in}$ stands for the total input intensity and $I_i^{\rm out}$ for the total output intensity that we observe. It is obvious that $I_0^{\rm in} \neq 0$ for the incident beam and $I_i^{\rm in} = 0$ for the diffracted beams ($i \neq 0$).

With no assumption about the properties of $I_i(\mathbf{s}, x_\mathbf{s})$, the intensity can be integrated on the path

$$I_i(\mathbf{s}, l_\mathbf{s}) = \int_0^{l_\mathbf{s}} \frac{\rm d}{{\rm d}x} I_i(\mathbf{s}, x)\,{\rm d}x + I_i(\mathbf{s}, 0). \tag{19}$$

Consequently, the integration over the cross section S can be written as

$$\int_S I_i(\mathbf{s}, l_\mathbf{s})\,{\rm d}\mathbf{s} = \int_S \int_0^{l_\mathbf{s}} \frac{\rm d}{{\rm d}x} I_i(\mathbf{s}, x)\,{\rm d}x\,{\rm d}\mathbf{s} + \int_S I_i(\mathbf{s}, 0)\,{\rm d}\mathbf{s}. \tag{20}$$

The integration of the first term on the right-hand side covers the whole volume V of the crystal; the path hence no longer needs to be specified by $\mathbf{s}$. With the boundary conditions (18), a simple expression for the whole crystal is obtained:

$$I_i^{\rm out} = \int_V \frac{\partial}{\partial x_i} I_i(\mathbf{r})\,{\rm d}\mathbf{r} + I_i^{\rm in}. \tag{21}$$

Substituting (17) into (21), we get the final integral equation:

$$I_i^{\rm out} = -\left(\mu + \sum_{j\neq i} r_{ji}\right) \int_V I_i\,{\rm d}\mathbf{r} + \sum_{j\neq i} r_{ij} \int_V I_j\,{\rm d}\mathbf{r} + I_i^{\rm in}. \tag{22}$$

Note that every integral in this equation depends neither on the beam direction nor on the path length.

The algebraic notation used in the previous section is effective again. We introduce internal-intensity vector $\mathbf{I}^V$ which consists of the intensity field integrated over the volume of the crystal as follows:

$$I_i^V \equiv \int_V I_i(\mathbf{r})\,{\rm d}\mathbf{r}. \tag{23}$$

Thereby, we can rewrite (22) as

$$\mathbf{I}^{\rm out} = \mathbf{T}\mathbf{I}^V + \mathbf{I}^{\rm in}, \tag{24}$$

where the matrix $\mathbf{T}$ is revised to be

$$T_{ij} \equiv r_{ij} - \delta_{ij}\left(\mu + \sum_{k=0}^{n-1} r_{kj}\right). \tag{25}$$

Equation (24), as a result of the integration of the intensity transfer equations over a small crystal, has the same form as (6) of the macroscopic formulae, but differs in $\mathbf{I}^V$.

To match these two equations, we propose an assumption: the internal-intensity vector $\mathbf{I}^V$ is coupled with the output intensity $\mathbf{I}^{\rm out}$ by an arbitrary operator $\mathbf{C}$ as

$$\mathbf{I}^V = \mathbf{C}\mathbf{I}^{\rm out}. \tag{26}$$

By this assumption, (24) can be rewritten as

$$\mathbf{I}^{\rm out} = \mathbf{T}\mathbf{C}\mathbf{I}^{\rm out} + \mathbf{I}^{\rm in}, \tag{27}$$

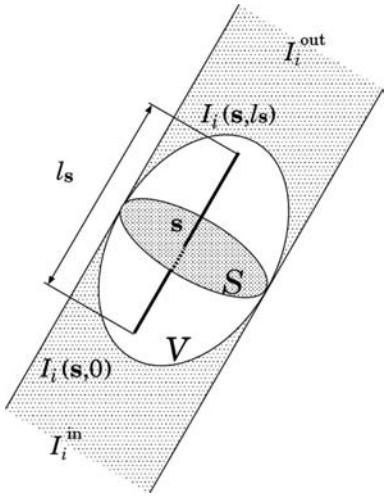

Figure 4
An integration path along the ith beam is schematically illustrated for a small crystal that is fully bathed in the incident beam. The position $\mathbf{s}$ on the cross section S specifies the path and its length $l_\mathbf{s}$. The intensities at both the boundaries of the path can be written as $I_i(\mathbf{s}, 0)$ and $I_i(\mathbf{s}, l_\mathbf{s})$.

which is almost equivalent to the results of the previous section. Consequently, the output intensities can be derived by (10), where $\mathbf{D} = \mathbf{E} - \mathbf{TC}$.

The operator $\mathbf{C}$ is the key to connecting the macroscopic formulae with the intensity transfer equations as a microscopic formulation. Dimensional analysis requires that the dimension of $\mathbf{C}$ must be $[L]$. It may contain information about the size and form of the specimen crystal, and may even be a linear operator written as a matrix. But we never expect that its expression can be determined by any experiment because we cannot measure the internal intensity fields directly. In the original method by Soejima *et al.* (1985), the transmission factor $r_{\mathbf{h}}$ may contain such information although treated as a scalar. Thus the method can be regarded as a simplified case that the operator $\mathbf{C}$ becomes a scalar C, *i.e.*

$$\mathbf{I}^V = C\mathbf{I}^{\text{out}}. \tag{28}$$

The constant value C may be hidden in the N_{ij}, then (6) and (27) become completely equal. As a result, we can state that the foundation of the macroscopic formulae is this hypothesis (28), which means that the observed intensity is proportional to the total integral of the internal intensity field of the beam in the crystal.

3. Discussion

To demonstrate this method, an application program *nbeam* has been developed for the numerical simulation of the ψ-scan experiment invented by Renninger (1937). By a ψ scan, the diffraction intensity modulated by the n-beam effect is recorded during the azimuthal rotation of the specimen crystal around the primary diffraction vector $\mathbf{h}_1$, namely the ψ axis. By simulation of the ψ rotation on a four-circle diffractometer with convergent and monochromatic incident X-rays (Busing & Levy, 1967), the program can calculate the n-beam diffraction intensity on the basis of (27) and the hypothesis (28) at each ψ angle where the cross sections r_{ij} of the relevant secondary lattice points are evaluated from the geometry in the reciprocal space.

In the present discussion, we focus on the two parameters C and μ; all the technical details of the ψ-scan simulation, including the evaluation of the r_{ij} with the Lp factor and apparatus functions, is described in a separate article (Nagao, 2005).

We select Si as a specimen because of the extinction rule by the diamond glide, for which the Renninger effect was originally found. Setting parameters are determined according to the lattice constant $a = 5.431028$ Å, by assuming [100] is parallel to the φ axis of a four-circle diffractometer with unpolarized incident X-rays of Fe $K\alpha$. The origin of ψ is defined by the bisecting position of the primary diffraction. In this case, the probability of n-beam diffraction is not so large that the n-beam effect appears as discrete peaks or dips on a ψ-scan profile.

The structure factors and μ are computed by the analytical method (Waasmaier & Kirfel, 1995) with the anomalous dispersion coefficients (Sasaki, 1989).

Fig. 5 shows an example of the ψ-scan calculation. *Umweganregung* peaks appear as a result of the n-beam effect on the 222 diffraction that is forbidden for the space group of diamond. The dotted line represents the profile for $\mu = 277$ cm^{-1}, which is the linear absorption coefficient for Fe $K\alpha$, and the solid line that for no absorption ($\mu = 0$). Both the calculations are carried out for $C = 1.0$ cm, then normalized at the maximum point ($\psi = 13.928^\circ$) to compare their profiles with a large difference in the peak height. The peaks are due to a ten-beam diffraction by eight secondary lattice points of which ψ angles are slightly different from each other. However, the $\mathbf{T}$ matrix is sparse because of the extinction rule due to the crystal symmetry. The main contributions to the left and right peaks are those from $1\bar{1}\bar{1}$ and from $5\bar{1}\bar{1}$, respectively. The variation of the peak height is derived from the similar calculations achieved for large ranges of C and μ. The results displayed in Fig. 6 indicate that the n-beam effect increases with increasing size of the specimen, and with decreasing μ.

Fig. 7 shows the Si 111 profile as another example of the ψ-scan simulation. The intensity of the primary diffraction is large; thus some dips caused by the *Aufhellung* effect can be

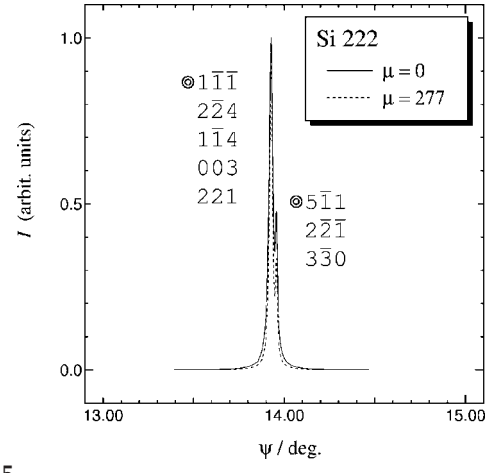

Figure 5
ψ-scan profiles of the Si 222 diffraction calculated for $C = 1.0$ cm. The solid and dotted lines respectively represent the cases for $\mu = 0$ and $\mu = 277$ cm^{-1}. The intensities are normalized at the peak position to compare profiles that differ in order of magnitude. The secondary lattice points denoted by the figures coincidentally have close ψ angles and produce the two *Umweganregung* peaks. The left peak mainly comes from $1\bar{1}\bar{1}$ and the right one from $5\bar{1}1$.

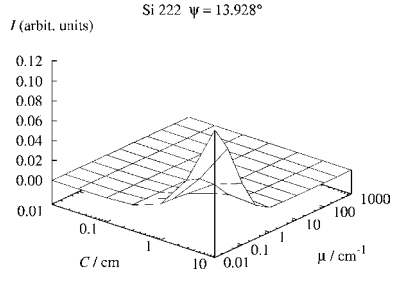

Figure 6
The peak intensity in the C–μ space for $\psi = 13.928^\circ$ in Fig. 5. The peak is higher in the region with large C and small μ.

seen. The first and second dips from the left are the results of the three-beam cases with one secondary diffraction.

Although the diffractions on the secondary lattice points $2\bar{4}0$ and $4\bar{2}0$ are not allowed by the extinction rule, the diffractions from the primary to secondary lattice point, *i.e.* $1\bar{5}\bar{1}$ and $3\bar{3}\bar{1}$, respectively, have finite values of the crystal structure factor, and hence cause the effects.

The deepest dip is from the six secondary lattice points that coincidentally have almost the same ψ angles, but only $\bar{1}\bar{1}1$ is effective with its corresponding diffraction $\bar{2}\bar{2}0$. The intensity profiles given by solid and dotted lines for $\mu = 0$ and 277 cm^{-1}, respectively, are normalized at $\psi = 0.0^\circ$. In contrast with the *Umweganregung* peak for Si 222 shown in Fig. 5, the dips for $\mu = 277$ cm^{-1} are hardly observed. Fig. 8 shows how the relative depth of the dip at $\psi = 2.680^\circ$ changes when C and μ are varied. The dip is remarkable in the region with large C and small μ.

These examples show that the magnitude of the n-beam effect depends on the specimen size and the absorption of the specimen. For large absorption, we expect that the *Aufhellung* dip would be difficult to measure, whereas the *Umweganregung* peak can be distinguished from the low base intensity. From the viewpoint of reducing the n-beam effect for the precise crystal structure analysis, the results indicate that a smaller crystal has an advantage for the same μC. It is also confirmed that the *Umweganregung* peak may happen to break the extinction rule even for a small crystal with large μ, where the n-beam effect is negligible.

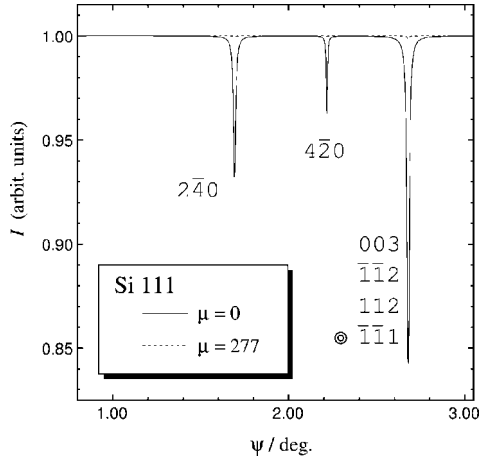

Figure 7
ψ-scan profiles of Si 111 calculated for $C = 1.0$ cm. The solid and dotted lines correspond to the cases $\mu = 0$ and $\mu = 277$ cm^{-1}, respectively. Both the profiles are normalized at $\psi = 0^\circ$. The n-beam effect appears as dips by *Aufhellung* because the primary reflectivity is large.

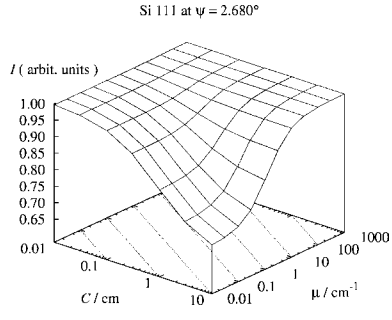

Figure 8
The Si 111 intensity in the C–μ space affected by the *Aufhellung* effect. The surface displays the variation of the intensity at $\psi = 2.680^\circ$ relative to that at $\psi = 0^\circ$. Dotted lines on the base show the direction in which μC is constant. The depth of the dip is shallow for large μ or small C; therefore, a smaller crystal is recommended to reduce both the n-beam and absorption effects.

4. Conclusions

Macroscopic intensity equations in the n-beam case have been derived from the intensity transfer equations based on the partial differential equations for small spherical crystals. With the proposed hypothesis given in (28), it is confirmed that the equations can be solved by numerical calculation. The example simulations of the ψ scan show reasonable intensity behaviour while the crystal size and the linear absorption coefficient are varied, indicating that the theory is useful to estimate the effect of phase-independent n-beam diffraction intensity.

The author is grateful to Professor A. Okazaki for many helpful discussions. He also acknowledges the help of Helsinki University of Technology which allowed him to complete the present paper.

References

Authier, A. (2003). *Dynamical Theory of X-ray Diffraction*, Revised ed. Oxford University Press.
Becker, P. J. & Coppens, P. (1974). *Acta Cryst.* A**30**, 129–147.
Busing, W. R. & Levy, H. A. (1967). *Acta Cryst.* **22**, 457–464.
Chang, S.-L. (1984). *Multiple Diffraction of X-rays in Crystals.* Berlin: Springer-Verlag.
Coppens, P. (1968). *Acta Cryst.* A**24**, 253.
Hauback, B. C., Mo, F. & Thorkildsen, G. (1990). *Aust. J. Phys.* **43**, 77–91.
Mazzocchi, V. L. & Parente, C. B. R. (1994). *J. Appl. Cryst.* **27**, 475–481.
Moon, R. M. & Shull, C. G. (1964). *Acta Cryst.* **17**, 805–812.
Nagao, S. (2005). in preparation.
Okazaki, A., Ohe, H. & Soejima, Y. (1988). *Aust. J. Phys.* **41**, 511–517.
Okazaki, A., Soejima, Y., Machida, M. & Ohe, H. (1988). *Acta Cryst.* B**44**, 568–575.
Okitsu, K. (2003). *Acta Cryst.* A**59**, 235–244.
Parente, C. B. R. & Caticha-Ellis, S. (1974). *Jpn. J. Appl. Phys.* **13**, 1501–1505.
Parente, C. B. R., Mazzocchi, V. L. & Pimentel, F. J. F. (1994). *J. Appl. Cryst.* **27**, 463–474.
Renninger, M. (1937). *Z. Phys.* **106**, 141.
Sasaki, S. (1989). *KEK Rep.* **88-14**, 1–136.
Soejima, Y., Okazaki, A. & Matsumoto, T. (1985). *Acta Cryst.* A**41**, 128–133.
Tanaka, K., Kumazawa, S., Tsumokawa, M., Maruno, S. & Shirotani, I. (1994). *Acta Cryst.* A**50**, 246–252.
Tanaka, K. & Saito, Y. (1975). *Acta Cryst.* A**31**, 841–845.
Thorkildsen, G. & Larsen, H. B. (2002). *Acta Cryst.* A**58**, 252–258.
Waasmaier, D. & Kirfel, A. (1995). *Acta Cryst.* A**51**, 416–431.
Zachariasen, W. H. (1965). *Acta Cryst.* **18**, 705–710.